Available online at www.sciencedirect.com
SCIENCE DIRECT®
Journal of Nuclear Materials 337–339 (2005) 985–989
journal of nuclear materials
www.elsevier.com/locate/jnucmat

Carbon chemical erosion in H-mode discharges in ASDEX Upgrade divertor IIb: flux dependence and local redeposition

R. Pugno [a,*], K. Krieger [a], A. Kirschner [b], A. Kallenbach [a], D.P. Coster [a], R. Dux [a], U. Fantz [a], J. Likonen [c], H.W. Müller [a], J. Neuhauser [a], V. Rohde [a], E. Vainonen-Ahlgren [c], ASDEX Upgrade Team

[a] *Max-Planck-Institut für Plasmaphysik, IPP–EURATOM Association, Boltzmannstrasse.2, D-85748 Garching, Germany*
[b] *Institut für Plasmaphysik, Forschungzentrum Jülich GmbH, EURATOM Association, Trilateral Euregio Cluster, D-52425 Jülich, Germany*
[c] *VTT Processes, Association EURATOM-Tekes, P.O. Box 1608, 02044 VTT, Finland*

Abstract

Carbon erosion at the outboard divertor in ASDEX Upgrade has been investigated using the emission spectroscopy technique. The methane molecular influx was calibrated by simultaneous CD_4 puffing. In deuterium H-mode discharges a decrease of $D/XB_{CD\leftarrow CD_4}$ with increasing ion flux (decreasing temperature) is found at fluxes in the range $0.5–2\times10^{22}\ m^{-2}\ s^{-1}$ and no dependence for higher fluxes. The corresponding obtained yields show a negative power law flux dependence with exponent $\gamma = -0.46$. To investigate the combined effect of re-deposition, re-erosion and local transport, known quantities of $^{13}CH_4$ were puffed at the end of the 2002/2003 experimental campaign. The amount of ^{13}C locally redeposited has been measured by nuclear reaction analysis (NRA). The results show a strongly localised re-deposition near the puff location, with a downstream tail and a moderate downward drift with respect to the magnetic field line direction.

PACS: 52.40.H; 52.25.V; 33.20.K
Keywords: ASDEX-Upgrade; Chemical erosion; Erosion and deposition; Spectroscopy; Surface analysis

1. Introduction

Carbon fiber composite is a candidate material for the ITER divertor target plates because of the good thermal and mechanical properties and its low atomic charge Z. Critical questions remain concerning its compatibility with tritium operation. The major obstacle is the chemical erosion of carbon via hydrocarbon formation, which may lead to co-deposition of hydrogen isotopes in hydrogen-rich carbon layers on plasma facing or even remote surfaces [1]. If this process cannot be suppressed in ITER, the use of carbon during the D–T phase would require active tritium removal techniques

* Corresponding author. Tel.: +49 89 32992571; fax: +49 89 32991812.
E-mail address: roberto.pugno@ipp.mpg.de (R. Pugno).

0022-3115/$ - see front matter © 2004 Published by Elsevier B.V.
doi:10.1016/j.jnucmat.2004.09.053

due to the small tritium inventory allowed for safety reasons. Therefore a better understanding of the erosion (primary and re-erosion), local transport and re-deposition is necessary.

The D/XB method, extension for the molecules of the S/XB method [2], is used in the following to obtain erosion yields at high fluxes, but its utilisation presents two problems: first the D/XB coefficients for hydrocarbon molecules and their dependence on plasma parameters are not well known and, secondly, no information is obtained about the amount of released hydrocarbon which is promptly re-deposited on the surface.

The first problem can be solved by means of simultaneous calibration puffing and by applying the obtained D/XB to the intrinsic photon fluxes [3–5]. The hydrocarbon re-deposition has been investigated by analysing the 2-D ^{13}C density distribution on the tile surface after localised $^{13}CH_4$ puffing.

2. Flux dependence of the D/XB value and of the erosion yield

2.1. Measurements

In the ASDEX Upgrade divertor, an absolutely calibrated diagnostic injection system has been installed. Dedicated wide angle line-of-sights (LOS) centred on the valve [VOU in Fig. 1] permit collecting the photons emitted from the molecules during the puff. An array of parallel LOS [RON in Fig. 1] covering a similar poloidal section (but at a different toroidal location) permits the unperturbed intrinsic emission to be measured. The radiation is measured with a 1 m Czerny–Turner spectrometer equipped with a 1200 l/mm grating. A 512×512 CCD camera coupled to the spectrometer permits to measure simultaneously 10 channels with a resolution of 0.015 nm/pixel over a spectral range of 7.7 nm. The typical CCD integration time is 50 ms, resulting in ELM averaged measurements.

$D/XB_{CD\leftarrow CD_4}$ and the resulting yields have been measured in standard H-mode discharges (run routinely at the beginning of each experimental day) and in few dedicated H-mode discharges, where a vertical scan of the plasma column has been performed to increase the investigated flux range. During the dedicated shots, feedback control on the neutral density in the divertor permitted stable plasma behaviour in the divertor.

Time integrated spectra of the identical shots 18460 and 18462 are shown in Fig. 2 and Fig. 3, respectively. The intrinsic contribution to the intensity during the puff is always less than 10% and its contribution in the D/XB calculation has been neglected. In some cases the contribution of the D_γ wings intensity to the CD band was as strong as the CD signal itself. Therefore and due to a dark current drift during the acquisition, the signal in an 'almost line-free interval' (shadowed interval in Fig. 2) has been taken as background level in the analysed shots. During the puff, the valve neighbouring LOS (ROV016 and ROV018 in Fig. 1) do not observe any CD emission increase, indicating a vertical size of the emitting cloud < 10 mm. The cloud could be more elongated in toroidal direction due to the parallel transport of intermediate fragments of the fragmentation chain. Detailed 3D modelling of the puffing is ongoing.

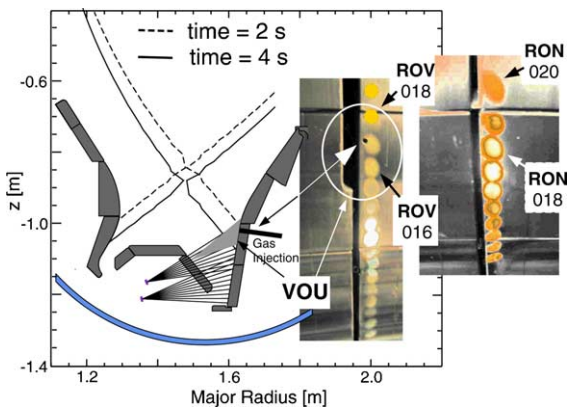

Fig. 1. Experimental arrangement in the divertor of ASDEX Upgrade. The bright spots on the tiles at the outboard target show the line-of-sight (LOS) positions: the LOS RON018 has been used to measure the unperturbed intrinsic CD photon fluxes from the wall. With a simultaneous puff, VOU measured $D/XB_{CD\leftarrow CD_4}$. The separatrix positions at two time points during the vertical scan are shown.

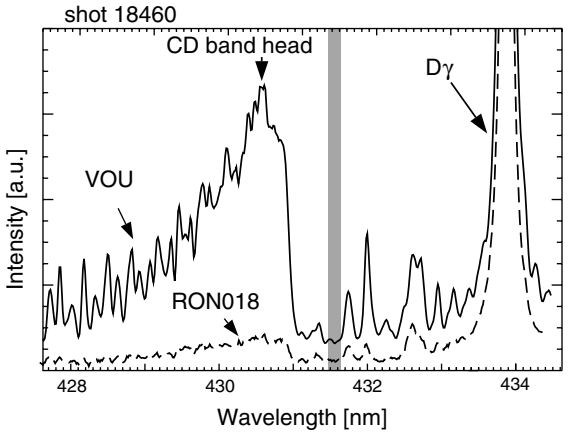

Fig. 2. Time integrated spectrum of the VOU and RON018 LOS during the puffing. The average value in the shadowed interval has been taken as background signal. Due to the different geometry of the two LOS, the signal are not directly comparable. The VOU observe the puffing cloud emission while RON measures only the intrinsic emission (being located at a different toroidal position).

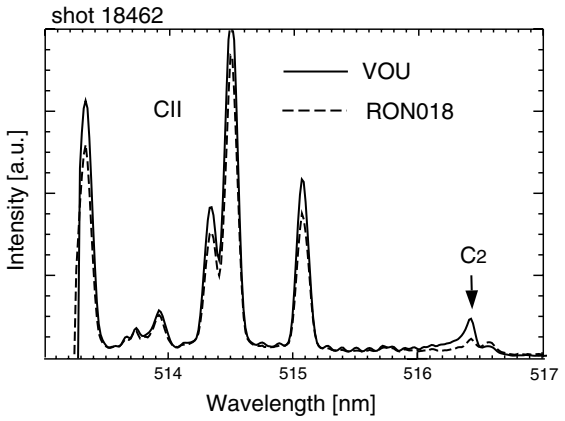

Fig. 3. Time integrated spectrum of the VOU and RON018 LOS during the puffing. Due to the different geometry of the two LOS the signal are not directly comparable. The VOU observe the puffing cloud emission while RON measures only the intrinsic emission (being located at a different toroidal position). To be noticed the increase of the C_2 emission due to the puff in comparison with the intrinsic C_2 emission.

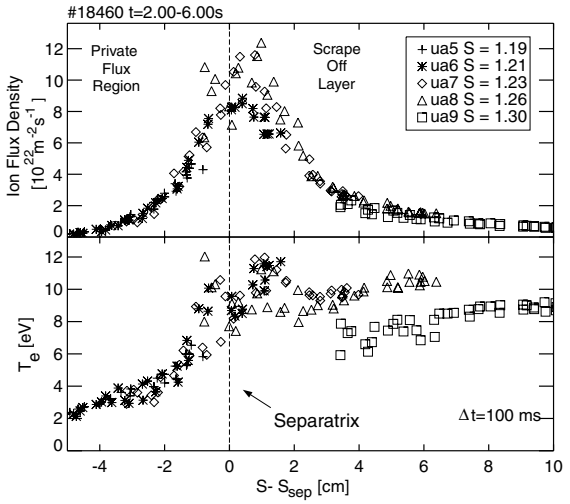

Fig. 5. Ion flux density and electron temperature profiles reconstructed from multiple probes during the plasma vertical shift as function of the distance along the target from the separatrix (S–S_{sep}). The data from the probe ua8 (triangles) are the measurements in poloidal proximity of the puffing location.

The radial penetration of the injected gas into the plasma before getting ionised is found to be <1 mm (see Section 3). The 7 cm diameter LOS VOU is expected to collect all photons emitted from the injected hydrocarbons into the observed solid angle.

The reconstruction of the intensity profiles of different emission lines (Fig. 4) and of the ion flux densities and electron temperatures (Fig. 5) show that the profiles stay self-similar during the vertical shift. Under these circumstances a single B2-EIRENE [6] calculation suffices as background plasma to model the puffing with ERO at different times during the discharge, i.e. at different plasma locations during the vertical shift. The Langmuir

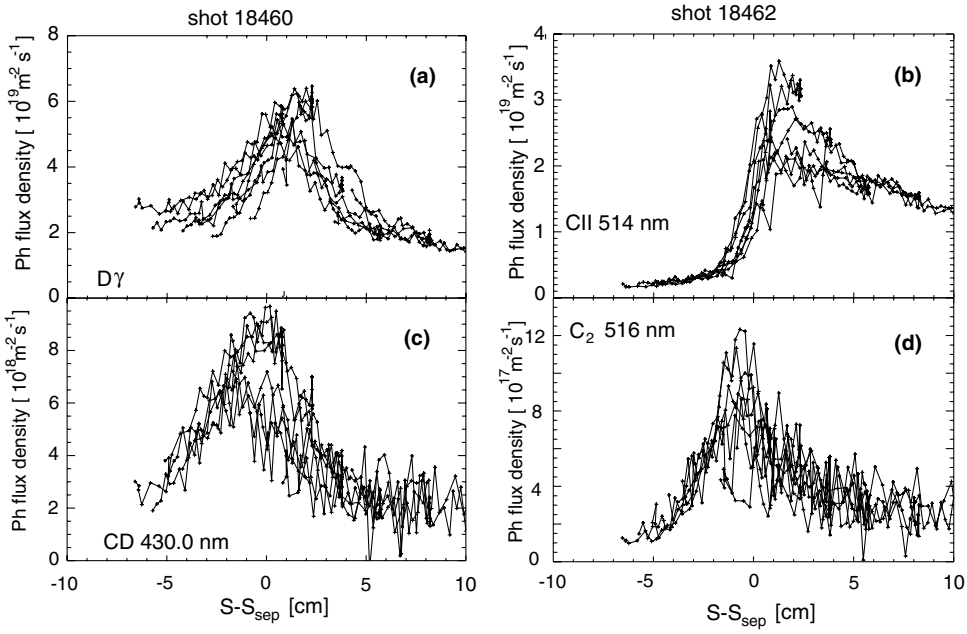

Fig. 4. Intrinsic intensity emission profiles reconstructed from multiple LOS (RON) during the plasma vertical shift as function of the distance along the target from the separatrix (S–S_{sep}): (a) Dγ, (b) CII at 514 nm, (c) CD band head (1.5 nm), and (d) C_2 at 516 nm.

probe ua8 is positioned near the puffing valve (in the poloidal section) and its measurements (triangles in Fig. 5) are taken as local plasma parameter during the puffing.

The typical parameters for the discharges analysed are: plasma current 1 MA, electron line-averaged density $5–8 \times 10^{19}\ m^{-3}$, neutral beam power 2.5–5 MW and CD_4 puff rate 3×10^{18} part/s. The target tile surface temperature varies between a minimum of 400 K to a maximum of about 600 K at the power density maximum, near the strike point [7].

2.2. Analysis

The measured $D/XB_{CD\leftarrow CD_4}$ (integrated over 1.5 nm) in H-mode (Fig. 6) decreases with increasing ion flux (decreasing temperature) for ion fluxes lower than $2 \times 10^{22}\ m^{-2}\ s^{-1}$ and shows no dependence for higher fluxes during each discharge (where $T_e \simeq$ constant). Typical values obtained are $D/XB_{CD\leftarrow CD_4} = 8–17$. The different $D/XB_{CD\leftarrow CD_4}$ values at similar ion fluxes for different shots result from different local electron temperatures at the puffing location: for $D/XB_{CD\leftarrow CD_4} \leqslant 12$ typical T_e = 6–8 eV are measured, while at higher local T_e (8–12 eV) the highest $D/XB_{CD\leftarrow CD_4}$ are obtained.

Applying the obtained D/XB to the intrinsic CD intensity measured from the LOS RON018 (Fig. 1), the CD_4 molecule flux density eroded from the wall is obtained. In Fig. 7 the erosion yields, calculated by dividing the molecule flux density by the ion flux density measured with a Langmuir probe, are shown.

The data can be described by a power law dependence, yield $\propto \Gamma^{\gamma}$, with $\gamma = -0.46$. This flux dependence is slightly weaker compared to an earlier study, where constant D/XB was assumed [8]. Including also ion beam experiment data for low ion fluxes, an improved fit is presented in [9,10], where the data are fitted by the formula: yield = $\text{yield}_{low}/(1 + (\Gamma/\Gamma_0)^c)$, where yield_{low} is the flux-independent yield at low fluxes and Γ_0 is the flux where the transition to flux dependence occurs.

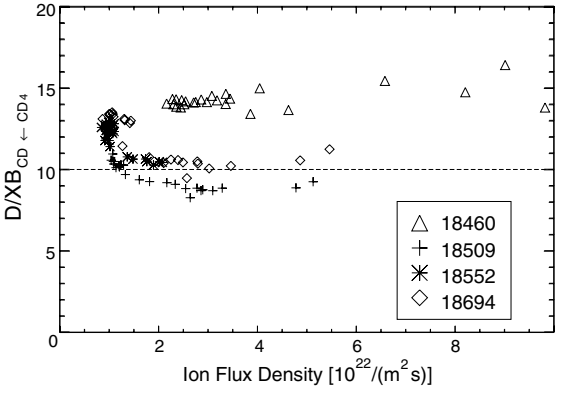

Fig. 6. The $D/XB_{CD\leftarrow CD_4}$ versus the ion flux density Γ.

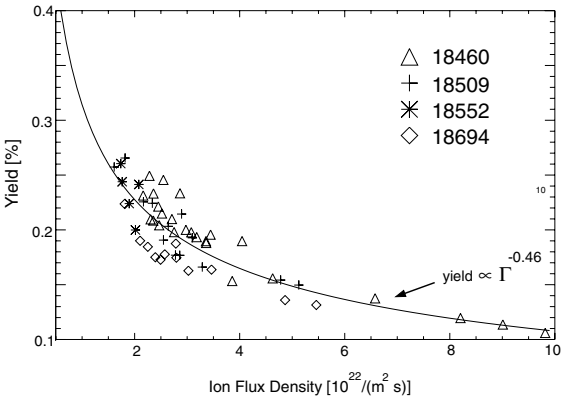

Fig. 7. The erosion yield versus the ion flux density Γ. The yield shows a power law dependence: yield $\propto \Gamma^{-0.46}$.

The total erosion yield, taking into account the contribution from higher hydrocarbons, is expected to be a factor 1.3–2 higher, as indicate by measurements in ASDEX Upgrade L-mode discharges and in laboratory plasmas [11].

3. ^{13}C redeposition

To obtain direct information on re-deposition and re-erosion probabilities of the CD_4/CH_4 particles leaving the wall, $^{13}CH_4$ has been injected during an H-mode shot repeated 12-times at the end of the 2002/2003 campaign. The main parameters of the discharge were: plasma current 1 MA, electron line-averaged density $8.5 \times 10^{19}\ m^{-3}$, neutral beam power 6.5 MW and $^{13}CH_4$ puff rate 3×10^{18} part/s. Between the repeated discharges 5 min He glow discharges were done. Their effect do not reach the lower divertor and no effect on the redeposited ^{13}C is expected. Afterwards, the puffing tile (Fig. 8(top)) was dismounted and the ^{13}C 2-D re-deposition map was measured via nuclear reaction analysis (p from $^3He(^{13}C,p)^{15}N$ using 2.4 MeV ^3He) (Fig. 8(bottom)).

The redeposition pattern follows approximately the magnetic field line direction, with an additional downward drift. The stronger downward drift near the valve, when the carbon ions result from ionisation closest to the wall, is probably caused by the $E \times B$ drift due to the pre-sheath and sheath potentials. Magnetic ray tracing shows that 1 cm in toroidal direction corresponds to a radial penetration of about 0.2 mm, i.e. about one Larmor radius, in front of the valve. The left edge of the tile is in the shadow of the adjacent upstream tile, and the puffing location is at the limit of the shadowed area. The higher ^{13}C density in the shadowed area

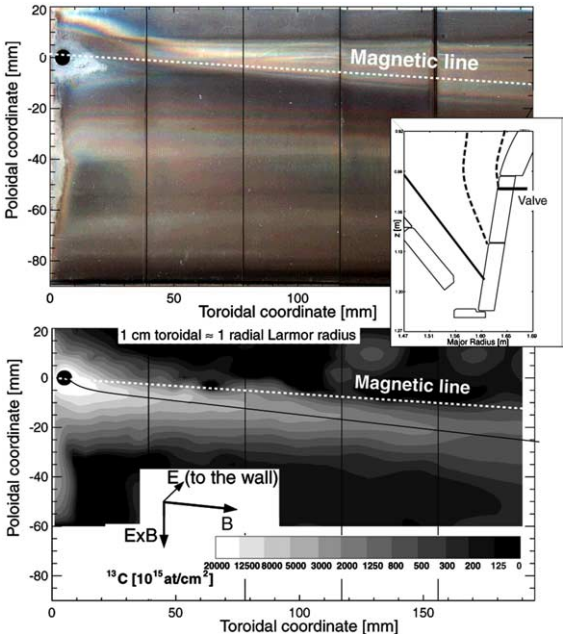

Fig. 8. Tile picture with the puffing hole (top) and ^{13}C density distribution (bottom). The redeposition tail maxima (black line) do not follow exactly the magnetic line direction. The strong downwards deviation in the first toroidal 15 mm from the valve (corresponding to 0.2 mm radially) is probably caused by the $E \times B$ drift due the pre-sheath and sheath potentials. In the small Figure (right) the separatrix and the valve positions at the outboard divertor for the pertinent discharges are shown.

indicates that part of the puffed gas can escape in the shadowed volume and diffuse more than the particles dragged away from the background plasma.

The total amount of redeposited ^{13}C (above the ^{13}C background level) is 1.3×10^{20} particles, to be compared with a total puffed ^{13}C atoms of 1.1×10^{20}. Within the experimental errors all the ^{13}C is reposited along a stripe starting from the puff location and extending no more than 18 cm. The deposition shows an exponential decay along a line curved toward the lower part of the divertor (black line, Fig. 8(bottom)).

4. Conclusion and outlook

The puff measurements show a decrease of $D/XB_{CD \leftarrow CD_4}$ with increasing ion flux (decreasing temperature) for fluxes lower than $2 \times 10^{22}\,m^{-2}\,s^{-1}$. For higher fluxes no flux dependence is evident, but discharges with lower local T_e and same ion flux density results in lower $D/XB_{CD \leftarrow CD_4}$. The resulting methane yield shows a power law dependence with ion flux density with $\gamma = -0.46$.

The total methane erosion yield in ASDEX Upgrade divertor IIb is found to be low with values of <0.3 %. The low yield is attributed to the effect of successive boronization, resulting in a reduction of the chemical erosion yield due to boron admixture in the surface layers [12].

At the end of the 2003/2004 campaign, more ^{13}C redeposition measurements are planned. Open questions remain about the impact/contribution of ELMs to the averaged values of D/XB and yields. High time resolution measurements, using interference filters and photomultipliers, are being tested in ASDEX Upgrade and are planned for the near future.

To understand the combined effects of fragmentation, excitation, ionisation (in the volume) and of the erosion and sticking (at the surface), modelling is necessary. As a first step, $D/XB_{CD \leftarrow CD_4}$ puffs in hydrogen L-mode discharges have been modelled with ERO code. Good agreement has been obtained between the modelling and the puffing measurements. Modelling of the presented hydrocarbon puff in H-mode discharges and of the local redeposition has been started. The results will be discussed in a following publication.

References

[1] G. Federici et al., J. Nucl. Mater. 290–293 (2001) 260.
[2] K. Behringer et al., J. Nucl. Mater. 176&177 (1990) 606.
[3] A. Pospieszczyk et al., Phys. Scr. T 81 (1999) 48.
[4] M.F. Stamp et al., Phys. Scr. T 91 (2001) 13.
[5] R. Pugno et al., in: Proceedings of the 30th Euro.Conf. on Contr. Fus. Plasma Phys., St. Petersburg, Russia, 2003.
[6] D.P. Coster et al., J. Nucl. Mater. 241–243 (1992) 690.
[7] A. Kirschner, V. Philipps, J. Winter, U. Kögler, Nucl. Fus. 40 (5) (2000) 989.
[8] A. Kallenbach et al., Phys. Scr. T 81 (1999) 43.
[9] J. Roth et al., these Proceedings. doi:10.1016/j.jnucmat.2004.10.115.
[10] J. Roth et al., Nucl. Fus., to be published.
[11] U. Fantz et al., these Proceedings. doi:10.1016/j.jnucmat.2004.10.044.
[12] D.G. Whyte et al., Phys. Scr. T 91 (2001) 7.